Title

Microbial composition of biofilms associated with lithifying rubble of Acropora palmata branches

Journal

FEMS Microbiology Ecology, 92(1)

ISSN

0168-6496

Authors

Beltrán, Yislem

Cerqueda-García, Daniel

Taş, Neslihan

et al.

Publication Date

2016

DOI

10.1093/femsec/fiv162

Microbial composition of biofilms associated with lithifying rubble of *Acropora palmata* branches

Yislem Beltran[1], Daniel Cerqueda-Garcıa[1], Neslihan Tas[2], Patricia E Thome[3], Roberto Iglesias-Prieto[3] and Luisa I. Falcon[1]*

[1]Laboratorio de Ecologıa Bacteriana, Instituto de Ecologia, UNAM, DF, Mexico, 04510, [2]Lawrence Berkeley National Laboratory, Earth & Environmental Sciences, Ecology Department, Berkeley, CA 94720, USA and [3]Unidad Academica de Sistemas Arrecifales, Puerto Morelos, Instituto de Ciencias del Mar y Limnologıa, UNAM Ado. Post. 1152, Cancun, QR, Mexico, 77500

∗ E-mail: falcon@ecologia.unam.mx

Abstract

Coral reefs are amongst the most productive ecosystems on the planet, but are rapidly declining due to global warming-mediated changes in the oceans. Particularly for the Caribbean region, *Acropora* sp. stony corals have lost ~80% of their original coverage, resulting in vast extensions of dead coral rubble. We analysed the microbial composition of biofilms that colonize and lithify dead *A. palmata* rubble in the Mexican Caribbean and identified the microbial assemblages that can persist under scenarios of global change, including high temperature and low pH. Lithifying biofilms have a mineral composition that includes aragonite and magnesium calcite (16 mole% $MgCO_3$) and calcite, while the mineral phase corresponding to coral skeleton is basically aragonite. Microbial composition of the lithifying biofilms are different in comparison to surrounding biotopes, including a microbial mat, water column, sediments and live *A. palmata* microbiome. Significant shifts in biofilm composition were detected in samples incubated in mesocosms. The combined effect of low pH and increased temperature showed a strong effect after 2-week incubations for biofilm composition. Findings suggest that lithifying biofilms could remain as a secondary structure on reef rubble possibly impacting the functional role of coral reefs.

Keywords: *Acropora palmata*; microbial carbonates; lithifying biofilms; global warming; pH; genetic diversity

INTRODUCTION

Coral reefs are formed by calcium carbonate skeletons secreted by stony corals, and are amongst the most productive ecosystems on the planet. However, they are declining rapidly due to a combination of environmental change, overfishing, coral diseases and ocean acidification (Hoegh-Guldberg *et al*. 2007). Particularly in the Caribbean region, *Acropora* spp. stony corals used to be the most abundant and most important species in terms of accretion of reef structure. However, since the early 1980s, *Acropora* spp. have suffered an excessive loss of individuals in several areas of the Caribbean (Aronson and Precht 2001), particularly due to disease, bleaching and storms (Rodriguez-Martinez, Banaszak and Jordan-Dahlgren 2001;

Patterson *et al*. 2002; Precht *et al*. 2002; Williams and Miller 2005). Despite fossil record evidence that coral reefs have had cycles of high diversity and extinction associated with large-scale environmental perturbations since the early Cambrian (Budd 2000), paleontological data suggest that accelerated mortality of *Acropora* spp. has not been significant since their first fossil record dated in the Late Oligocene (Budd 2000; Aronson and Precht 2001), up until two decades ago (Rodriguez-Martinez *et al*. 2014).

Paleobiological studies indicate that coral reef taphonomy (post-mortem history of biological material including skeletal) is of importance since carbonate skeleton is altered via physical, chemical and biological processes that impact its composition and preservation (Greenstein and Pandolfi 2003). Coral reefs form wide ridges of reef rubble in highly disturbed areas. This rubble is often composed of material derived from the dead branches of colonial coral (in the case of *A. palmata*) that originates from the reef front. It has been suggested that when coral is broken on the reef front, it can accumulate *in situ* and then can be transported to form rubble ridges in the reef lagoon, resulting in a permanent cycle of coral destruction and regeneration (Blanchon, Jones and Kalbfleisch 1997). This cycle will produce structures that are built up by successive layers of coral rubble over thousands of years (Blanchon, Jones and Kalbfleisch 1997; Thornborough and Davies 2011). Lithification by either biological or physical cement that stabilizes a secondary reef structure is involved in the composition and preservation of rubble (Rasser and Riegl 2002).

Although coral reefs are one of the most important and oldest carbonate frameworks in the world, bacterial carbonates (e.g. stromatolites) were important reef builders long before eukaryotes appeared (Hofmann 2000). Prokaryotes can induce carbonate precipitation by their metabolic activity (Dupraz *et al*. 2009). Metabolisms that induce mineral precipitation in bacteria are sulfate reduction, denitrification, urea hydrolysis (Visscher, Reid and Bebout 2000; Hammes *et al*. 2003; Fujita *et al*. 2008) and photosynthesis (Arp, Reimer and Reitner 2001). Carbonate precipitation can also be influenced by passive organic interaction between the geochemical environment and bacteria (Dupraz *et al*. 2009). Microbial calcification often takes place in a biofilm of layers of organic matter (extracellular polymeric substances) attached to substrates that contain a variety of bacteria within a matrix of degrading organic matter, where it can be an important binding or cementing agent (Riding 2000). The fossil record indicates that numerous coral reef frameworks are formed by large volumes of bacterial crust (Westphal *et al*. 2010) some of which persist today in tropical shallow-water reefs (Camoin *et al*. 2012). These reef-bacterial crusts have been called cements, stromatolites and microbialites, and are mainly composed of magnesium calcite (Riding, Liang and Braga 2014), playing an important role in reef development not only by contributing a significant amount of carbonate to the primary reef structure but also by aiding in the stabilization and binding of the reef framework. Calcareous encrusting communities can

influence preservation of a primary framework built by corals, developing a secondary reef framework (Perry and Hepbum 2008).

After the great decline of reef-building *A. palmata* in the Mexican Caribbean, dead coral rubble colonized by microbial communities is a common occurrence. Although microbial lithification may be relevant in the reef, its role in binding of rubble and healthy coral tissue has not yet been described (Ainsworth, Thurber and Gates 2010). This study presents the first survey of biofilms that grow and cement *A. palmata* rubble, and microbial aggregates inhabiting seawater and liquid–solid interface biotopes associated with rubble ridges in the Mexican Caribbean. Biofilms growing and cementing *A. palmata* rubble are described following a high-throughput 16S rRNA itag-MiSeq sequencing strategy to identify the microbial assemblages that may prevail under scenarios of global change (Caporaso *et al*. 2010), represented in different mesocosm systems, including the isolated and combined effects of high temperature and low pH at different incubation times.

MATERIALS AND METHODS

Study area and sampling

Puerto Morelos is located 32 km south of Cancun, Mexico, 20° 48′–20° 52′ N and 86° 51′–86° 55′ W (Fig. 1). The barrier reef runs along the entire coastline with a length of 15 km, and is part of the Mesoamerican Barrier Reef. The reef lagoon has a width of 550–1500 m and 3–5 m depth. Lagoon seawater is oligotrophic with low nitrite (0.06 µg-at L^{-1}), nitrate (13.9 µg-at L^{-1}) and phosphate (0.46 µg-at L^{-1}). Salinity varies little throughout the year (35.8 to 36.2 ups). The average value of registered alkalinity is 2.5 mEq L^{-1}, and pH of 8.3; average surface water temperature ranges between 25.1 and 29.9°C (Merino and Otero 1991). The dry and rainy seasons are not clearly defined and the hurricane season extends from June through November (Rodriguez-Martinez *et al*. 2010).

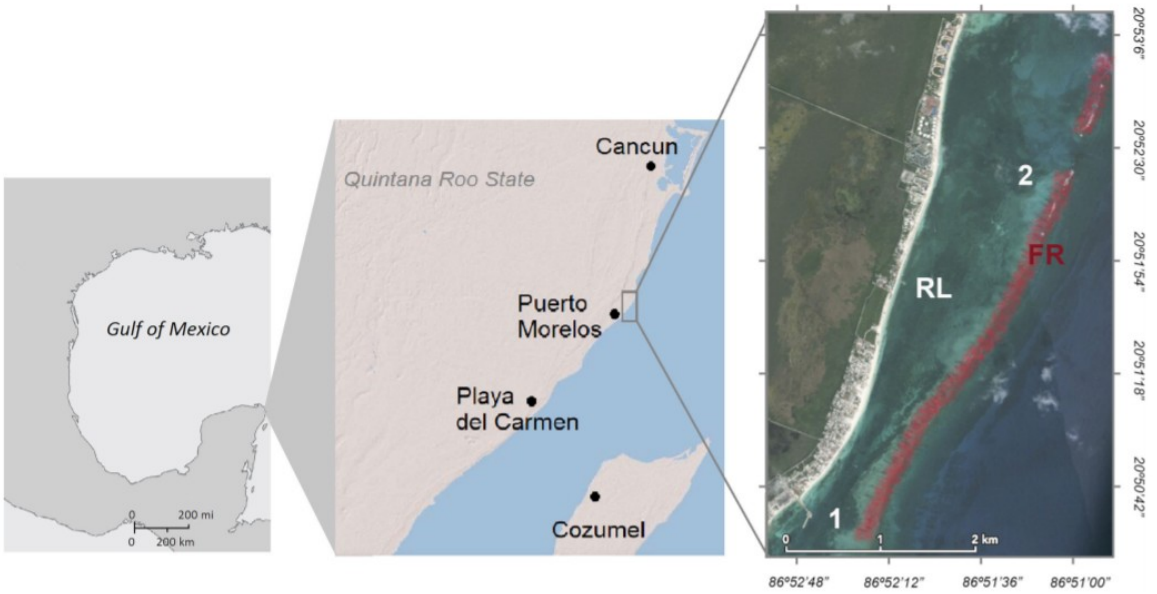

Figure 1. Geographical location of study area in the Puerto Morelos reef system on the eastern coast of the Yucatan Peninsula, Mexico. RL: reef lagoon; 1: lagoon sampling station of different biotopes; 2: lagoon sampling site 'La Bocana'; FR: fringing reef.

In June 2013 *Acropora palmata* rubble, undergoing two different stages of biofilm growth (Fig. 2) (Stage 1, biofilm without lithification; Stage 2, lithified biofilm) were collected from the reef lagoon in Puerto Morelos (~5 m depth). Biofilms were collected by apnea with hammer and chisel and brought back to the laboratory in a cooler. Samples of ~5 cm^2 of the uppermost surface of the rubble were stored at −20°C in the laboratory. Stage 1 biofilm is a microbial aggregate growing on *A. palmata* carbonate substrate, where calcified biofilm is thinner and cementation of the rubble is weak. Stage 2 biofilm exhibits a complex structure, with a strong degree of cementation that binds rubble together. Samples of different biotopes adjacent to *A. palmata* rubble were collected to analyse their microbial diversity and compared to rubble biofilms, including sediment, overlying seawater, a microbial mat and live tissue of *A. palmata*. Sediment samples were collected in triplicate with 10 cm cores adjacent (30–60 cm) to sampled rubble and stored in sterile bags. Seawater overlying the rubble was collected in triplicate with sterile 1 L containers. A microbial mat growing in proximity to the sampled area was also collected in triplicate with sterile 10 cm cores. A sample of *A. palmata* tissue was collected by removing ~2 cm^2 of the uppermost 1 cm of a coral colony with a sterile chisel. Samples were kept in sterile containers in darkness and frozen at −20°C until analysis. Rubble was analysed using a stereomicroscope to identify structural differences between Stage 1 and 2 biofilms, at the Institute of Biology, UNAM. Mineral characterization of biofilms on rubble and *A. palmata* skeleton was obtained by powder X-ray diffraction (Empyrean, PANalytical B.V.) at the Institute of Geology, UNAM.

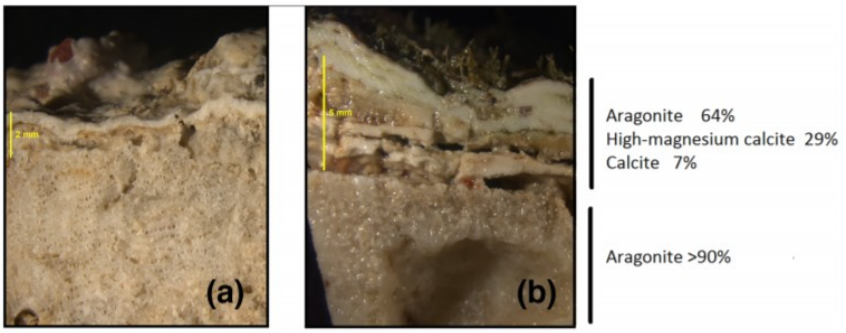

Figure 2. Stereomicroscopic images representing Stage 1 (a) and Stage 2, lithified (b) biofilms growing on *A. palmata* rubble collected from the Puerto Morelos reef, Mexico. Mineral composition of biofilms and coral obtained with X-ray diffraction is shown.

DNA extraction

Total environmental DNA was extracted from each type of sample (n = 6 per biofilms, n = 3 per biotope described above) following the protocol of Zhou, Bruns and Tiedje (1996) with modifications. We used a homogenized mixture of 5 g for each sample, which was pulverized on ceramic mortars with liquid nitrogen and 9 mL of extraction buffer (100 mM Tris-HCl, 1.5 M NaCl, 100 mM EDTA, 100 mM Na_3PO_4, pH 8). The freeze–thaw and continuous maceration cycle was repeated three times. Samples were incubated for 30 min at 37°C with lysozyme (1 mg mL^{-1} final concentration), cetyltrimethylammonium bromide (CTAB 6%) and left overnight at 55°C with a volume of 20% sodium dodecyl sulphate (SDS) and proteinase K (0.1 mg mL^{-1} final concentration). Samples were extracted twice with phenol:chloroform:isoamyl alcohol (25:24:1) and once with chloroform, recovering the supernatant after each centrifugation (8000 r.p.m. for 20 min). DNA was precipitated by addition of 0.6 volume of chilled absolute ethanol, 1/10 volume of 3 M sodium acetate and refrigerated at −20°C overnight. DNA was recovered by centrifugation (3500 g for 20 min) and the pellet was washed with 70% ethanol (all reagents came from Sigma-Aldrich, St Louise, MO, USA). The DNA pellet was further purified with a DNeasy Blood & Tissue kit following the protocol of the manufacturer (Qiagen) and resuspended in molecular grade water. Water samples were thawed and filtered through Durapore membranes (0.22 µm) (Millipore). DNA from filters was extracted as described above.

Mesocosms

In order to assess the response of biofilms to changes in temperature and pH we used a mesocosm system. Fragments of lithified biofilm-covered *A. palmata* rubble were collected in August 2013 in the Puerto Morelos reef as described above. The sampling site is known as ‘La Bocana’ (20° 52′ 20.92′ N, 86° 51′ 12.52′ W), and represents an area where extensive colonization of *A. palmata* rubble with lithified biofilms occurs. Samples were transported immediately after collection to the mesocosm system, which consisted of four 60 L capacity open top tanks, screened with several layers of netting to remove 75% of natural illumination. The mesocosm system was designed as

follows: control: re-creating the temperature (30°C) and pH (8.2) of the seawater in the sampling site; high temperature: increased temperature by 2°C, control pH value of 8.2; low pH: decrease in pH to 7.9, control temperature of 30°C; combined: high temperature (32°C), low pH (7.9). Triplicate samples of 5 cm^2 of the uppermost surface of the incubated fragments were taken for each treatment at several time points: at the beginning of the experiment (immediately after leaving them in tanks) and after 1, 3, 7, 11 and 15 days of incubation. Total DNA for these samples was extracted as described above. pH in mesocosms was adjusted by bubbling CO_2 into flowing seawater, and temperature was controlled using a recirculating chiller, until reaching experimental values (pH 7.9, pCO_2 = 890 p.p.m.; pH 8.2, pCO_2 = 390 p.p.m.). Both parameters were monitored with an AquaController System (Neptune Systems, San Jose, CA, USA).

16S rRNA gene amplification and sequencing

A 420 bp fragment including the V4 hypervariable region of the 16S rRNA gene was PCR-amplified following the protocol of Caporaso *et al*. (2012) for paired-end community sequencing using universal primers 515F/806R for Bacteria and Archaea. PCR for each sample had a specific Golay reverse primer (Caporaso *et al*. 2010). DNA concentration was calculated from each sample with a Qubit dsDNA HS assay (Invitrogen), and ~2 ng μl^{-1} of total DNA was used in PCR reactions consisting of a final volume of 25 µl, 2.5 µl Takara ExTaq PCR 10× buffer (TaKaRa Corp., Shiga, Japan), 2 µl Takara dNTP mix (2.5 mM), 0.7 µl bovine serum albumin (20 mg ml^{-1}, Roche), forward and reverse primers (0.2 µM final concentration), 0.125 µl Takara Ex Taq DNA Polymerase (5 u μl^{-1}) and nuclease-free water (Sigma-Aldrich). Thermal cycling conditions included an initial denaturation step at 95°C for 3 min, followed by 35 cycles of denaturation at 95°C for 30 s, primer annealing at 52°C for 40 s, strand extension at 72°C for 90 s and a final extension step at 72°C for 12 min. Three PCR reactions for each biotope sample were combined and purified with the SPRI magnetic bead, AgencourtAMPure XP PCR purification system (Beckman Coulter, Brea, CA, USA), and DNA concentration of each sample, after pooling PCR products, was obtained with the Qubit dsDNA HS assay. Amplicons were pooled (~20 ng per sample, identified with a specific Golay reverse primer) and sequenced on the Illumina MiSeq300 platform (at the Yale Center for Genome Analysis, CT, USA), resulting in ~250 bp paired end reads. The length of short reads was extended by overlapping paired-ends using FLASH (Magoc and Salzberg 2011). Quality filtering and demultiplexing were performed in QIIME (r = 1; p = 0.75; q = 3; n = 0, min_count 0.005) as described by Caporaso *et al*. (2012) and Bokulich *et al*. (2013), identifying the first quality score below Q3 and truncating the read prior to that position. Reads retained were those with at least 75% of the length of the input sequence and without any ambiguous base calls. USEARCH (Edgar 2010) was used to group sequences into operational taxonomic units (OTUs) at 97% similarity and also remove chimeric sequences. Taxonomic assignments for each OTU were given in

QIIME (Caporaso *et al*. 2012) version 1.7.0 using RDP classifier (Wang *et al*. 2007) and Greengenes database release 13_5. Phylogenetic trees were generated using FastTree2 (Price, Dehal and Arkin 2010) with QIIME's default parameters; these trees were used for diversity metrics. The sequence data generated and used in this study were deposited in the European Nucleotide Archive SRA under project ID PRJEB10076.

Diversity, richness and Good's coverage metrics were calculated using QIIME with non-phylogenetic analysis on a single OTU table file. β diversity was calculated by weighted UniFrac distance metrics. The weighted UniFrac distance matrix was used to obtain the ordination of the whole composition detected by 16S rRNA gene amplicon sequencing in a distance-based redundancy analysis (db-RDA) (Legendre and Legendre 1998). This RDA analysis was conducted in QIIME to test statistical significance of sample grouping. All cluster analysis to group samples with similar composition were made by the UPGMA method based on Bray–Curtis distance and plotted with the 'cluster' package in R 3.2.2.

For the mesocosm experiments, a principal components analysis (PCA) based on composition differences at the genus level (L6) amongst sites was plotted in R using the vegan 2.2-1 and Biodiversity R 2.5-3 packages. An equilibrium circle was drawn on the ordination plot, where the genera that contribute significantly to the ordination have vectors outside of the circle (Legendre and Legendre 1998).

RESULTS AND DISCUSSION

Rubble composed of materials derived from dead *Acropora palmata* branches showed under stereomicroscopic observations a lithified matrix associated with the biofilms (Fig. 2a and b), which impedes fragments to be separated. Mineral characterization by X-ray diffraction showed that the biofilm is composed of a mixture of aragonite with magnesium calcite (16 mole% $MgCO_3$) and calcite, while the mineral phase corresponding to coral skeleton found in the inner phase of the rubble is basically aragonite. Similar reefal non-skeletal lithification has been reported in the geological outcrop (Camoin *et al*. 1999). The microbially induced mineralization consisting of laminar fine-grained crusts has been described as cements, microbial crusts, stromatolites and microbialites, and are common features of sedimentary structures of reefal facies (Camoin *et al*. 1999; Braissant *et al*. 2003; Riding and Tomas 2006; Camoin, Iryu and McInroy 2007; Riding, Liang and Braga 2014). This binding overgrowth consists of microbial carbonates produced by bacterial communities (Rasser and Riegl 2002) and coralline algae, and has been acknowledged to be crucial in coral reefs for the edification and stabilization of substrates (Riding, Martin and Braga 1991). Bacterial carbonates suggest an adhesive biofilm where calcified bacterial organic matter and grains are trapped in a crust. The surface of this microbial biofilm can trap sediments and provide a medium for $CaCO_3$ precipitation (Riding 2011). Microbial crust is considered the last stage of reef formation and the

most abundant. In most cores obtained in geological sections, microbially induced mineralization is a major structural and volumetric component of reefs, constituting up to 80% of the rock (Camoin *et al*. 1999; Riding 2002). The mineral forms precipitated by biological activity can be distinguished from inorganic minerals by their chemical and structural heterogeneity. Specifically, calcite may contain up to 30% $MgCO_3$ and high amounts of Na, SO_4, H_2O, OH– and HCO_3 (Tucker 1990). Within shallow marine tropical waters the main carbonate mineralogies are Mg-calcites (containing 14–20 mol% $MgCO_3$), which are more abundant than aragonite in reefs (Perry and Hepbum 2008). The mineralogy found in bacterial carbonates is a solid solution of high-Mg calcite with 11–17% Mg^{2+} (Dupraz *et al*. 2009). Therefore, the lithified biofilm identified growing on the rubble of *A. palmata* branches (Fig. 2b), could consist of a secondary carbonate framework, originated from the biological precipitation of carbonates by microbially induced mineralization. This new framework of carbonate allows resilience of the substrate that reef builders including coralline algae and corals can use as a substrate to grow on.

A total of 2 862 324 sequences were obtained from six biotopes (Stage 1 and lithified biofilms, healthy coral, microbial mat, water and sediments adjacent to Stage 1 and lithified biofilms). Samples were rarefied to 14 400 sequences and grouped in a total of 12 668 OTUs at 97% of similarity. The biotope with the lowest number of OTUs was the healthy *A. palmata* coral (466 OTUs), while the largest number of OTUs was found in the Stage 1 biofilm (3493 OTUs). Diversity was highest in Stage 1 biofilms, sediments and microbial mats, followed by lithified biofilms. Water, and healthy corals had the lowest diversity (Table 1); Good's coverage was on average 90% for all biotopes. High diversity of calcified microbial communities has previously been recorded in reef systems (Papineau *et al*. 2005, 2008; Ley *et al*. 2006), although this is the first attempt to characterize the biofilms that lithify *A. palmata* rubble.

Table 1. Estimated richness indices (OTU, Chao1, ACE), diversity indices (H′, EH, Simpson) and coverage for all biotopes.

Sample	No. of sequences	OTUs	Chao1	ACE	H′	E_H	Simpson	Good's coverage (%)
Stage 1 biofilm	110 738	3493	5910	6140	10.35	0.88	1	93
Stage 2 lithified biofilm	80 576	1983	3539	3620	8.72	0.8	0.99	90
Healthy *A. palmata*	67 319	466	583	589	3.17	0.36	0.61	99
Microbial mat	65 803	2800	4346	4494	9.66	0.84	0.99	95
Seawater	83 550	786	1410	1402	5.82	0.61	0.94	96
Sediment	155 441	3140	5499	5644	10.06	0.87	1	88

Sixty-four phyla were recovered from the entire biotope-associated bacterial composition including candidate phyla, with ~92% (depending of biotope) of the sequences affiliated to 14 phyla (Fig. 3a). Although composition between biotopes showed the same abundant phyla, their proportion varied among biotopes. Proteobacteria was the most abundant phylum in each biotope. Other ubiquitous phyla included Bacteroidetes, Planctomycetes, Cyanobacteria, Actinobacteria, Acidobacteria and Crenarchaeota, the last

particularly abundant in rubble biofilms. Distance-based redundancy (db-RDA) analysis of ecological distance by ordination revealed that the compositions of the biotopes analysed here were different from each other (pseudo-$F_{10, 18}$ = 10.36, $P < 0.001$) (Fig. 3b). This analysis identified each biotope as a significant explanatory variable of spatial genetic variation after 999 permutations, explaining 85% of total variance, suggesting that microbial aggregates are specific for each biotope. Clustering analysis of the microbial composition showed greater similarity within mineral-associated biotopes (Fig. 3c). Indeed, samples from Stage 1 and lithified biofilms had a more similar composition among them and sediments than to any other biotope included in this study, indicating the strong shift in composition between healthy coral and the biofilms that colonize their remains and form a secondary reef structure.

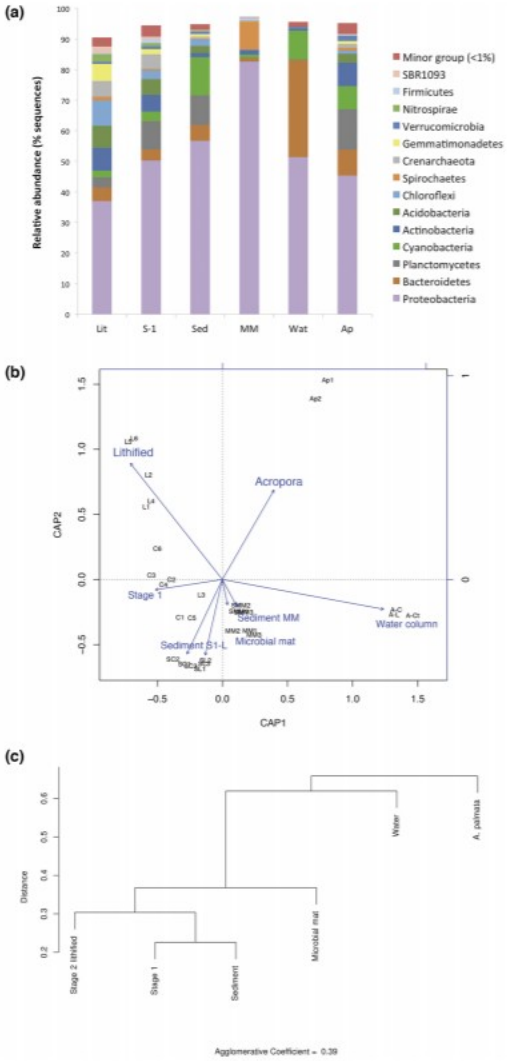

Figure 3. Comparison of bacterial taxonomic composition in different biotopes associated with *A. palmata* rubble. (**a**) Dominating phyla abundance per biotope: Stage 1, biofilm (S-1); Stage 2, lithified biofilm (Lit); microbial mat (MM); healthy *A. palmata* (Ap); overlying seawater (Wat); sediment (Sed). (**b**) Distance-based redundancy (db-RDA) analysis of ecological distance by ordination. (**c**) Clustering UPGMA showing distance relationships among biotopes, based on Bray–Curtis distance matrix.

Healthy *A. palmata* bacterial composition was predominantly characterized by abundance (Fig. 3a) of Proteobacteria, Bacteroidetes, Planctomycetes and to a lesser extent Cyanobacteria and Actinobacteria. A similar composition has been registered in the live tissue of corals (Frias-Lopez *et al*. 2002; Rohwer *et al*. 2002; Pantos and Bythell 2006; Nithyanand and Pandian 2009). Water sample controls had a typical composition of communities from overlying seawater (Frias-Lopez *et al*. 2002) highlighting the presence of Proteobacteria, Bacteroidetes and Cyanobacteria. In addition to Proteobacterial dominance, microbial mat composition was characterized by a greater proportion of Cyanobacteria (Fig. 3a). The compositions of the biofilms and microbial mat are similar to bacterial biofilms associated with carbonates (Papineau *et al*. 2005; Havemann and Foster 2008; Centeno *et al*. 2012). Biofilms colonizing *A. palmata* rubble showed the relevance of Proteobacteria, Bacteroidetes, Planctomycetes, Actinobacteria, Crenarchaeota, Acidobacteria and Chloroflexi as the most abundant phyla (Fig. 3a).

The lithified biofilm had 17 dominant classes, representing 80% of total abundance (Fig. 4). Classes representing abundances <1% are shown in Supplementary Fig. S1. Chloroplasts have a common ancestor within the Cyanobacteria (Falcón, Magallón and Castillo 2010); the 16S rRNA amplification protocol can identify chloroplast diversity that in this study corresponded to Chlorophyta, Rhodophyta and Stramenopiles. Presence of coralline algae is supported by mineral composition of biofilms, where calcite and magnesium calcite are relevant components (Stanley, Ries and Hardie 2002), and is consistent with reports that show coralline algae as secondary-framework builders after coral disturbance (Perry and Hepbum 2008).

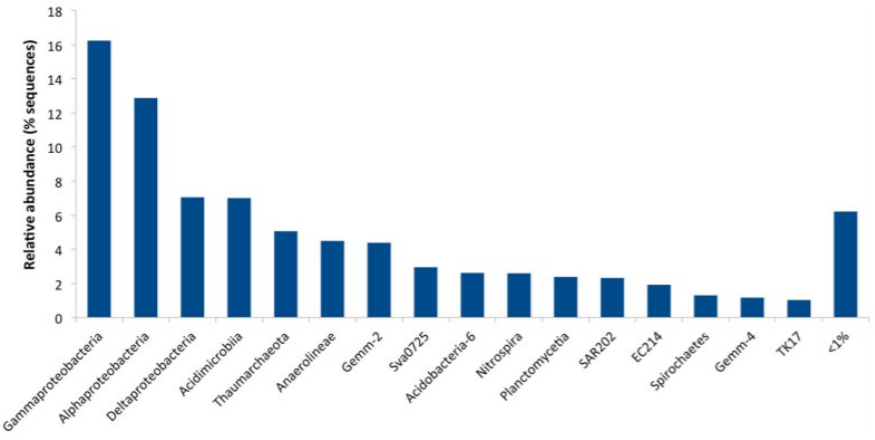

Figure 4. Distribution of most abundant microbial classes (relative abundance >1%) identified in the lithified biofilm. Remaining classes with low relative abundance have been grouped in the <1% bar.

Mesocosm experiments on lithified biofilms

A total of 7 593 586 high-quality sequences were obtained for all four treatments maintained in the mesocosm system, ranging from 48 436 to 184 388 sequences per sample, which were rarified to 48 400. Microbial

composition of lithified rubble in a PCA ordination of each experimental set-up for each set of pH and temperature conditions showed a clear division in microbial composition between samples incubated at least 1 week or less (1, 3, 7 incubations days) and composition of samples for the second week of the experiment (11 and 15 incubation days) (Fig. 5a) (individual PCA figures for each mesocosm condition are shown in Supplementary Fig. S2). UPGMA clustering shows that composition is more similar between samples during the first week and for the second week, respectively by clustering day 11 and 15 outwardly of days 0, 1, 3 and 7 (Fig. 5b). PCA analysis suggests that ordination of samples incubated at least 1 week or less are conducted mostly by the composition of genera *Vibrio* and *Pseudoalteromonas*. A negative correlation relationship has been described by Rodrigues *et al*. (2015) who identified *Pseudoalteromonas* as a potential inhibitor of biofilm development, a negative correlation that also seems to be present in this dataset for the first week (Pearson's correlation $r = -0.73$), but statistical meaning is poor ($P = 0.27$) due to the small number of observations (days). Major changes in abundance between the first and second week were found in Gamma- and Alphaproteobacteria, Clostridia and Bacilli. Changes in distribution of abundance at the class level are shown (Fig. 6a), according to the time of incubation under the combined effect of temperature increase and pH decrease vs current conditions (30°C and pH 8.2). Gamma-, Alpha-, Delta- and Epsilonproteobacteria, Clostridia, Bacilli, Planctomycetia and Acidimicrobiia were the most abundant groups for Week 2. Differences in class distribution between control and combined low pH and high temperature conditions for Week 2 were found (Fig. 6b), highlighting the increase in Bacilli and Acidimicrobiia under the combined effect of temperature increase and low pH.

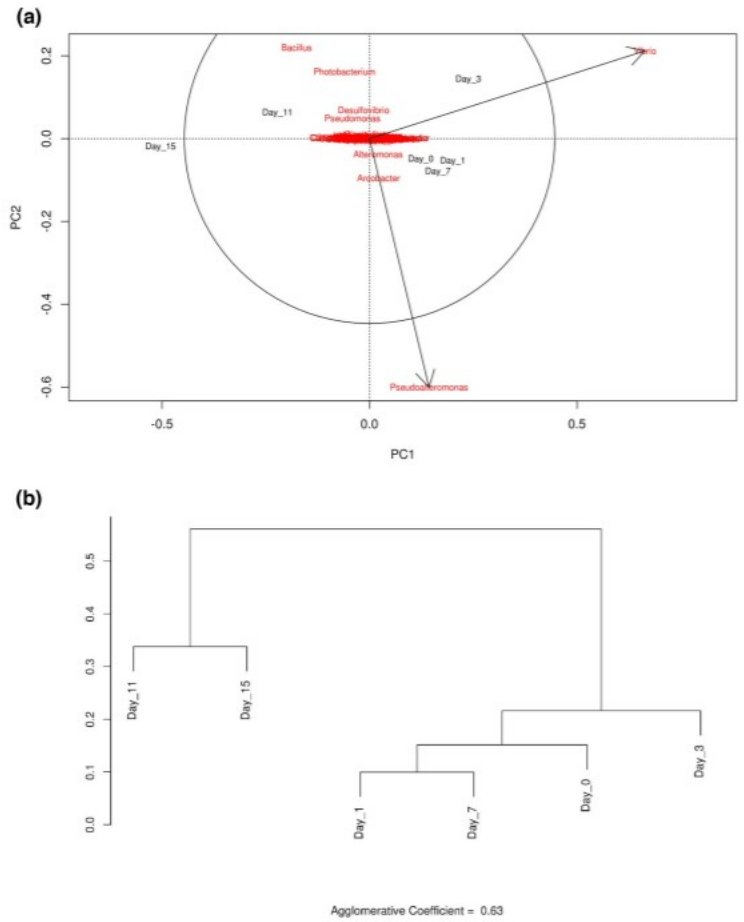

Figure 5. Bacterial diversity to genus level in the lithified biofilm representing different incubation times for the mesocosm condition with the combined effect of low pH and high temperature. (**a**) Principal components analysis (PCA) scaling to 1; the goodness of fit for the ordination was calculated by the percentage of variance explained for each day by the two first components, resulting in more than 70% per day (see Supplementary Table). An equilibrium contribution circle was drawn, where genera that contribute more to the ordination have vectors longer than the radius of the circle; the radius is equal to $\sqrt{d/p}$, where d is the number of dimensions and p is the total number of descriptors (Legendre and Legendre 1998). (**b**) Hierarchical clustering dendrogram by UPGMA (average linkage) method based on Bray–Curtis distance matrix, showing two principal groups for composition similarity; Day.11, 15 and Day.0, 1, 3, 7.

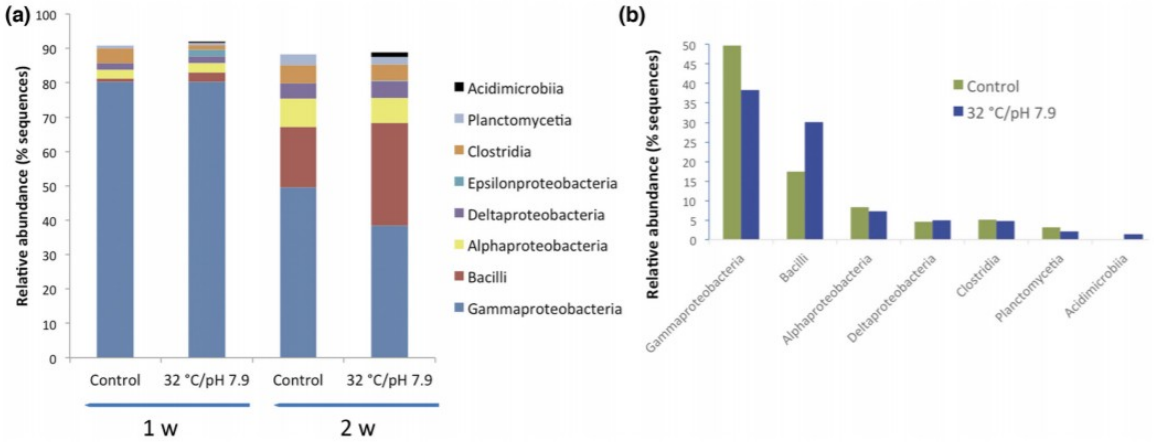

Figure 6. (**a**) Abundance distribution of the most representative classes (>1%) between the first and second week of incubation under control (pH 8.2/30°C) and combined mesocosms conditions (pH 7.9/32°C). (**b**) Class distribution in the second week between control and combined mesocosms conditions.

The results from the mesocosm experiments suggest that the variation in microbial composition is accentuated with time spent in the combined condition of 32°C and pH 7.9 where biofilms that colonize *A. palmata* rubble may be significantly modified under expected scenarios of changes in pH and temperature for the Mexican Mesoamerican Barrier Reef. The response of marine invertebrates and plankton to elevated CO_2 concentration has been investigated before (Hoegh-Guldberg *et al*. 2007; Newbold *et al*. 2012; Johnson *et al*. 2013). However, despite the importance of microbes for a coral reef ecosystem's function and health, there are just a few published studies of how decrease of pH by increased CO_2 concentrations can impact these key ecosystem players (Witt *et al*. 2011; Lidbury *et al*. 2012).

Experimental studies have focused on the effects of high CO_2 concentrations on bacterial communities in marine mesocosms showing scarce changes in composition for late century (~1140 p.p.m. of CO_2) scenarios (Liu *et al*. 2010; Witt *et al*. 2011; Lidbury *et al*. 2012; Roy *et al*. 2013). Roy and colleagues (2013) obtained a similar result on bacterial structure in pelagic communities using high-throughput 16S rRNA gene amplicon sequencing. Other works report no significant changes in microbial community structure (Tanaka *et al*. 2008; Newbold *et al*. 2012). Changes in the relative abundance of some phylotypes have been recorded under pCO_2 concentrations over 400 p.p.m. (Witt *et al*. 2011). A similar composition to that obtained in this study was reported in Arctic surface sediments exposed to different CO_2 concentrations, where some Proteobacterial classes, Chloroplasts and Planctomycetia dominated the microbial communities (Tait *et al*. 2013). Acidification experiments on Arctic microbial communities hint at shifts in taxa dominance and diversity under acidic conditions specifically for Acidimicrobiia (Monier *et al*. 2014). Some authors suggest that microorganisms associated with sediments are already adapted to low pH and fluctuating conditions experienced in microbial communities due to microbially mediated redox reactions (Zhu, Aller and Fan 2006; Joint, Doney and Karl 2011). Such has been the challenge of establishing the effect of acidification on microbial communities, where ongoing discussions hypothesize that since microbes already experience natural pH variations, processes other than calcification will not be fundamentally affected (Joint, Doney and Karl 2011); others argue that, based on meta-analysis, the rate of several microbial processes will be affected (Liu *et al*. 2010).

The response of the microbial composition associated with lithified rubble of *A. palmata* appears to support the hypothesis that predicted variations in pH and temperature will affect microbial colonization of altered coral reef ecosystems. In conclusion, this study represents the first attempt to characterize the biofilms that lithify *A. palmata* rubble, which consist of a secondary carbonate framework that could allow resilience of the substrate for further settlement of reef-builders including coralline algae and coral. Analysis of the response of microbial composition at elevated CO_2 levels indicates differences between current and projected conditions for the near

future, where predicted changes in pH and temperature appear relevant for these biofilms.

SUPPLEMENTARY DATA

Supplementary Data.

Sampling and mesocosms were conducted at UNAM's Coral Reef Academic Unit, in Puerto Morelos, Mexico. Technical support is acknowledged from O. Gaona, Susana Guzmán Gómez and F. Negrete-Soto. Mesocosm systems support is acknowledged from Dr W. Krämer and X-ray diffraction analysis support from Dr T. Pi Puig. This paper is part of the graduate degree requirements for YB, in the Posgrado en Ciencias Biológicas, UNAM. YB and DC-G are recipients of graduate studies fellowships (CONACyT). Funding was provided to LIF from SEP-CONACyT grant No. 0151796 and UNAM-PAPIIT grant No. 100212-3. All samples were collected under collector permit No. PPF/DGOPA-113/14 (LIF).

REFERENCES

Ainsworth TD, Thurber RV, Gates RD. The future of coral reefs: a microbial perspective. Trends Ecol Evol 2010;25:233–40.

Aronson RB, Precht WF. White-band disease and the changing face of Caribbean coral reefs. Hydrobiologia 2001;460:25–38.

Arp G, Reimer A, Reitner J. Photosynthesis-induced biofilm calcification and calcium concentrations in phanerozoic oceans. Science 2001;292:1701–4.

Blanchon P, Jones B, Kalbfleisch W. Anatomy of a fringing reef around Grand Cayman: storm rubble, not coral framework. J Sediment Res 1997;67:1–16.

Bokulich NA, Subramanian S, Faith JJ et al. Quality-filtering vastly improves diversity estimates from Illumina amplicon sequencing. Nat Methods 2013;10:57–9.

Braissant O, Cailleau G, Dupraz C et al. Bacterially induced mineralization of calcium carbonate in terrestrial environments: the role of exopolysaccharides and amino acids. J Sediment Res 2003;73:485–90.

Budd AF. Diversity and extinction in the Cenozoic history of Caribbean reefs. Coral Reefs 2000;19:25–35.

Camoin GF, Gautret P, Montaggioni LF et al. Nature and environmental significance of microbialites in Quaternary reefs: the Tahiti paradox. Sediment Geol 1999;126:271–304.

Camoin GF, Iryu Y, McInroy DB. IODP expedition 310 reconstructs sea level, climatic, and environmental changes in the South Pacific during the last deglaciation. Sci Drilling 2007;5:4–12.

Camoin GF, Seard C, Deschamps P et al. Reef response to sealevel and environmental changes during the last deglaciation: integrated Ocean Drilling Program Expedition 310, Tahiti Sea Level. Geology 2012;40:643–6.

Caporaso JG, Kuczynski J, Stombaugh J et al. QIIME allows analysis of high-throughput community sequencing data. Nat Methods 2010;7:335–6.

Caporaso JG, Lauber CL, Walters WA et al. Ultra-high-throughput microbial community analysis on the Illumina HiSeq and MiSeq platforms. ISME J 2012;6:1621–4.

Centeno CM, Legendre P, Beltran Y et al. Microbialite genetic diversity and composition relate to environmental variables. FEMS Microbiol Ecol 2012;82:724–35.

Dupraz C, Reid RP, Braissant O et al. Processes of carbonate precipitation in modern microbial mats. Earth Sci Rev 2009;96:141–62.

Edgar RC. Search and clustering orders of magnitude faster than BLAST. Bioinformatics 2010;26:2460–1.

Falcon LI, Magallon S, Castillo A. Dating the cyanobacterial ancestor of the chloroplast. ISME J 2010;4:777–83.

Frias-Lopez J, Zerkle AL, Bonheyo GT et al. Partitioning of bacterial communities between seawater and healthy, black band diseased, and dead coral surfaces. Appl Environ Microb 2002;68:2214–28.

Fujita Y, Taylor JL, Gresham TLT et al. Stimulation of microbial urea hydrolysis in groundwater to enhance calcite precipitation. Environ Sci Technol 2008;42:3025–32.

Greenstein BJ, Pandolfi JM. Taphonomic alteration of reef corals: effects of reef environment and coral growth form II: the Florida Keys. Palaios 2003;18:495–509.

Hammes F, Boon N, de Villiers J et al. Strain-specific ureolytic microbial calcium carbonate precipitation. Appl Environ Microb 2003;69:4901–9.

Havemann SA, Foster JS. Comparative characterization of the microbial diversities of an artificial microbialite model and a natural stromatolite. Appl Environ Microb 2008;74:7410–21.

Hoegh-Guldberg O, Mumby PJ, Hooten AJ et al. Coral reefs under rapid climate change and ocean acidification. Science 2007;318:1737–42.

Hofmann HJ. Archean stromatolites as microbial archives. Microbial Sedim 2000, 315–27.

Johnson VR, Brownlee C, Rickaby REM et al. Responses of marine benthic microalgae to elevated CO2. Mar Biol 2013;160: 1813–24.

Joint I, Doney SC, Karl DM. Will ocean acidification affect marine microbes? ISME J 2011;5:1–7.

Legendre P, Legendre L. Numerical Ecology. Amsterdam: Elsevier Science BV, 1998.

Ley RE, Harris JK, Wilcox J et al. Unexpected diversity and complexity of the Guerrero Negro hypersaline microbial mat. Appl Environ Microb 2006;72:3685–95.

Lidbury I, Johnson V, Hall-Spencer JM et al. Community-level response of coastal microbial biofilms to ocean acidification in a natural carbon dioxide vent ecosystem. Mar Pollut Bull 2012;64:1063–6.

Liu J, Weinbauer MG, Maier C et al. Effect of ocean acidification on microbial diversity and on microbe-driven biogeochemistry and ecosystem functioning. Aquat Microb Ecol 2010;61: 291–305.

Magoc T, Salzberg SL. FLASH: fast length adjustment of short reads to improve genome assemblies. Bioinformatics 2011;27:2957–63.

Merino M, Otero L. Atlas Ambiental Costero, Puerto MorelosQuintana Roo, Chetumal, Mexico: Centro de Investigaciones de Quintana Roo, 1991.

Monier A, Findlay HS, Charvet S et al. Late winter under ice pelagic microbial communities in the high Arctic Ocean and the impact of short-term exposure to elevated CO2 levels. Front Microbiol 2014;5:490.

Newbold LK, Oliver AE, Booth T et al. The response of marine picoplankton to ocean acidification. Environ Microbiol 2012;14:2293–307.

Nithyanand P, Pandian SK. Phylogenetic characterization of culturable bacterial diversity associated with the mucus and tissue of the coral Acropora digitifera from the Gulf of Mannar. FEMS Microbiol Ecol 2009;69:384–94.

Pantos O, Bythell JC. Bacterial community structure associated with white band disease in the elkhorn coral Acropora palmata determined using culture-independent 16S rRNA techniques. Dis Aquat Organ 2006;69:79–88.

Papineau D, Walker JJ, Mojzsis SJ et al. Composition and structure of microbial communities from stromatolites of Hamelin Pool in Shark Bay, Western Australia. Appl Environ Microb 2005;71:4822–32.

Patterson KL, Porter JW, Ritchie KE et al. The etiology of white pox, a lethal disease of the Caribbean elkhorn coral, Acropora palmata. Proc Natl Acad Sci U S A 2002;99:8725–30.

Perry CT, Hepbum LJ. Syn-depositional alteration of coral reef framework through bioerosion, encrustation and cementation: Taphonomic signatures of reef accretion and reef depositional events. Earth Sci Rev 2008;86:106–44.

Precht WF, Bruckner AW, Aronson RB et al. Endangered acroporid corals of the Caribbean. Coral Reefs 2002;21:41–2.

Price MN, Dehal PS, Arkin AP. FastTree 2–approximately maximum-likelihood trees for large alignments. PloS One 2010;5:e9490.

Pringault O, Duran R, Jacquet S et al. Temporal variations of microbial activity and diversity in marine tropical sediments (New Caledonia lagoon). Microbial Ecol 2008;55: 247–58.

Rasser MW, Riegl B. Holocene coral reef rubble and its binding agents. Coral Reefs 2002;21:57–72.

Riding R. Microbial carbonates: the geological record of calcified bacterial-algal mats and biofilms. Sedimentology 2000;47: 179–214.

Riding R. Biofilm architecture of Phanerozoic cryptic carbonate marine veneers. Geology 2002;30:31–4.

Riding R. Reefal microbial crusts. In: Hopley D (ed.). Encyclopedia of Modern Coral Reefs: Structure, Form and Process. Dordrecht: Springer, 2011, 911–5.

Riding R, Liang L, Braga JC. Millennial-scale ocean acidification and late Quaternary decline of cryptic bacterial crusts in tropical reefs. Geobiology 2014;12:387–405.

Riding R, Martin JM, Braga JC. Coral-stromatolite reef framework, upper Miocene, Almer´ıa, Spain. Sedimentology 1991;38:799– 818.

Riding R, Tomas S. Stromatolite reef crusts, Early Cretaceous, Spain: bacterial origin of in situ-precipitated peloid microspar? Sedimentology 2006;53:23–34.

Rodrigues S, Paillard C, Dufour A et al. Antibiofilm activity of the marine bacterium Pseudoalteromonas sp. 3J6 against Vibrio tapetis, the causative agent of brown ring disease. Probiotics Antimicrob Proteins 2015;7:45–51.

Rodriguez-Martinez RE, Banaszak AT, Jordan-Dahlgren E. Necrotic patches affect Acropora palmata (Scleractinia: acroporidae) in the Mexican Caribbean. Dis Aquat Organ 2001;47:229–34.

Rodriguez-Martinez RE, Banaszak AT, McField MD et al. Assessment of Acropora palmata in the Mesoamerican Reef System. PloS One 2014;9:e96140.

Rodriguez-Martinez RE, Ruiz-Renteria F, van Tussenbroek B et al. Environmentalstate and tendencies of the Puerto Morelos CARICOMP site, Mexico. Rev Biol Trop 2010;58:23–43.

Rohwer F, Seguritan V, Azam F et al. Diversity and distribution of coral-associated bacteria. Mar Ecol Prog Ser 2002;243: 1–10.

Roy AS, Gibbons SM, Schunck H et al. Ocean acidification shows negligible impacts on high-latitude bacterial community structure in coastal pelagic mesocosm. Biogeosciences 2013;10:555–66.

Stanley SM, Ries JB, Hardie LA. Low-magnesium calcite produced by coralline algae in seawater of Late Cretaceous composition. Proc Natl Acad Sci U S A 2002;99:15323–6.

Tait K, Laverock B, Shaw J et al. Minor impact of ocean acidification to the composition of the active microbial community in an Arctic sediment. Environ Microb Rep 2013;5:851–60.

Tanaka T, Thingstad TF, Lovdal T et al. Availability of phosphate for phytoplankton and bacteria and of glucose for bacteria at different pCO2 levels in a mesocosm study. Biogeosciences 2008;5:669–78.

Thornborough KJ, Davies PJ. Reef flats. In: Hopley D (ed.). Encyclopedia of Modern Coral Reefs: Structure, Form and Process. Dordrecht: Springer, 2011, 869–76.

Tucker ME, Bathurst RG (eds). Carbonate Diagenesis, Vol. 1. Oxford: Blackwell Scientific Publications, 1990.

Visscher PT, Reid RP, Bebout BM. Microscale observations of sulfate reduction: Correlation of microbial activity with lithified micritic laminae in modern marine stromatolites. Geology 2000;28:919–22.

Wang Q, Garrity GM, Tiedje JM et al. Naive Bayesian classifier for rapid assignment of rRNA sequences into the new bacterial taxonomy. Appl Environ Microb 2007;73:5261–7.

Westphal H, Heindel K, Brandano M et al. Genesis of microbialites as contemporaneous framework components of deglacial coral reefs, Tahiti (IODP 310). Facies 2010;56:337–52.

Williams DE, Miller MW. Coral disease outbreak: pattern, prevalence and transmission in Acropora cervicornis. MEPS 2005;301:119–28.

Witt V, Wild C, Anthony KRN et al. Effects of ocean acidification on microbial community composition of, and oxygen fluxes through, biofilms from the Great Barrier Reef. Environ Microbiol 2011;13:2976–89.

Zhou JZ, Bruns MA, Tiedje JM. DNA recovery from soils of diverse composition. Appl Environ Microb 1996;62:316–22.

Zhu Q, Aller RC, Fan Y. Two-dimensional pH distributions and dynamics in bioturbated marine sediments. Geochim Cosmochim Ac 2006;70:4933–49.